Electronic Supplementary Information

Paper-based Microfluidic Aluminum-Air Batteries: Toward Next-Generation Miniaturized Power Supply

Liu-Liu Shen [a], Gui-Rong Zhang [a,*], Markus Biesalski [b], and Bastian J.M. Etzold [a,*]

[a]Ernst-Berl-Institut für Technische und Makromolekulare Chemie, Department of Chemistry, Technische Universität Darmstadt, Alarich-Weiss-Straße 8, 64287 Darmstadt, Germany

[b]Laboratory of Macromolecular Chemistry and Paper Chemistry, Department of Chemistry, Technische Universität Darmstadt, Alarich-Weiss-Straße 8, 64287 Darmstadt, Germany

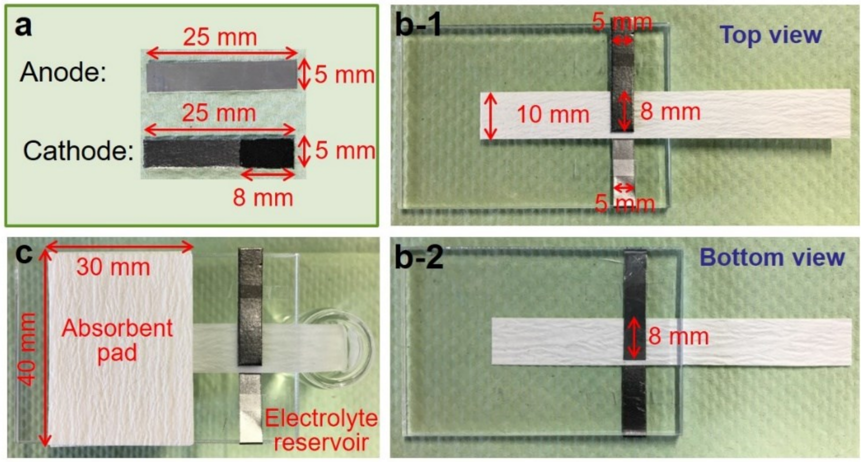

Fig. S1 (a) Dimensions of the anode and cathode electrodes. (b) Display of the prototypical paper-based μAl-air battery from top and bottom view. (c) A prototypical paper-based μAl-air battery during discharge.

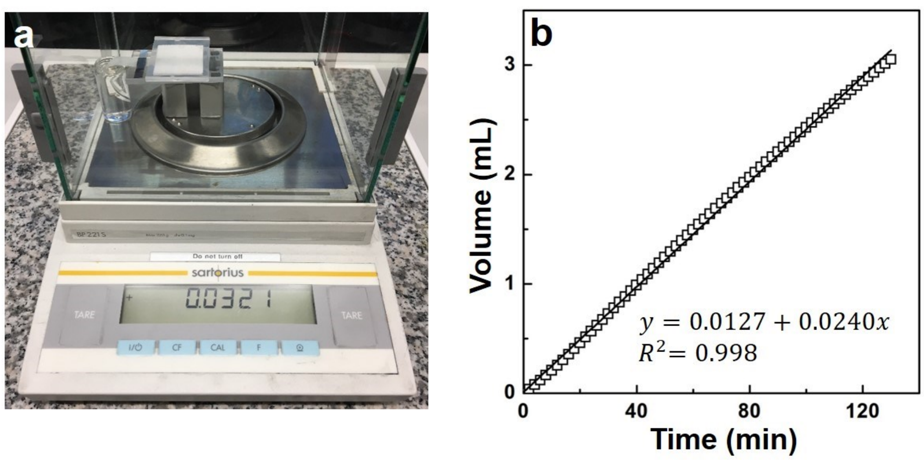

Fig. S2 (a) Flow rate measurement of the electrolyte (1.5 M KOH solution) on paper channel (VWR grade 417). (b) The volume of the electrolyte accumulated on absorbent pads was plotted against elapsed time. The flow rate calculated by linear regression is marked.

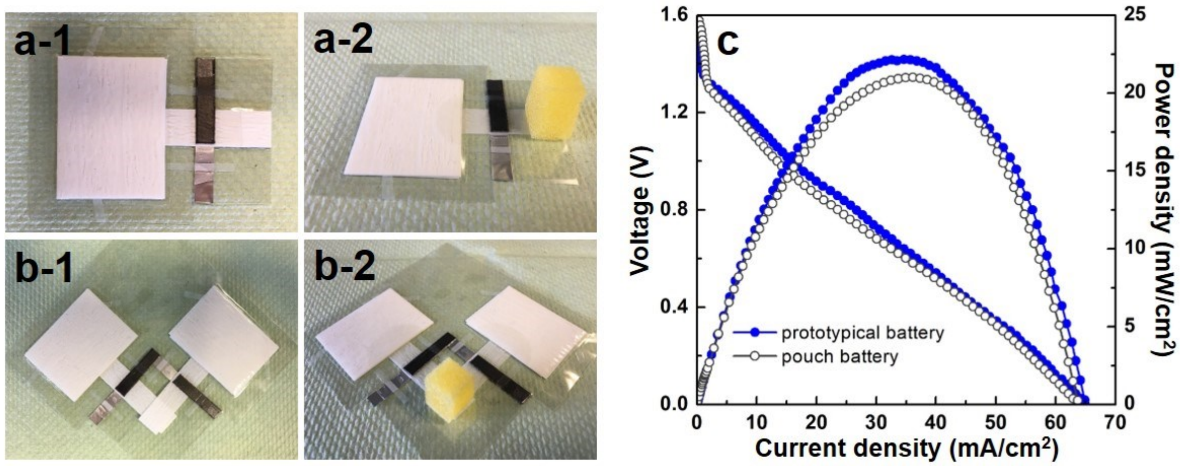

Fig. S3 A paper-based μAl-air pouch battery before (a-1) and during discharging (a-2). Two paper-based μAl-air pouch batteries connected in series before (b-1) and during discharging (b-2). (c) Polarization (*V-I*) and power density curve of a single paper-based μAl-air battery in pouch configuration.

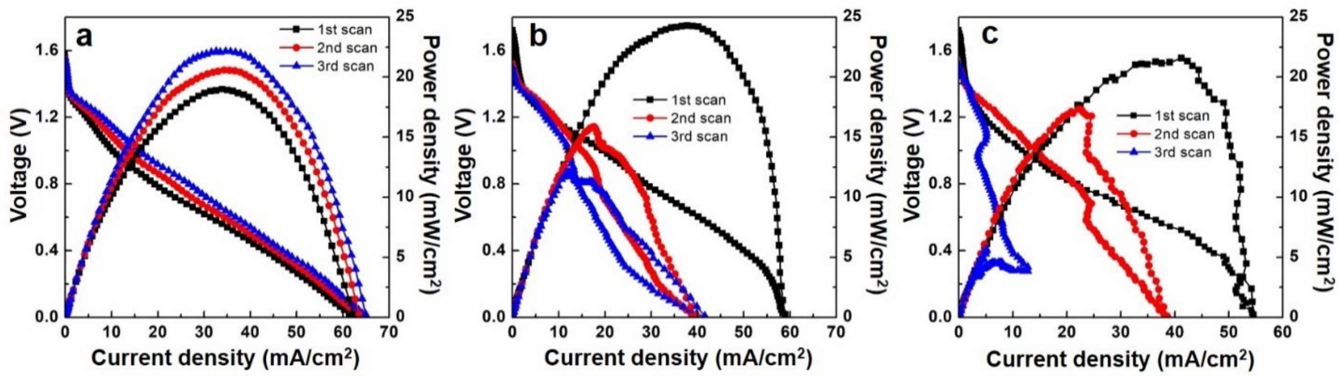

Fig. S4 Polarization (*V-I*) and power density curves of paper-based μAl-air battery with 1.5 M (a), 2.0 M (b) and 2.5 M (c) KOH solution by continuous staircase linear scan voltammetry.

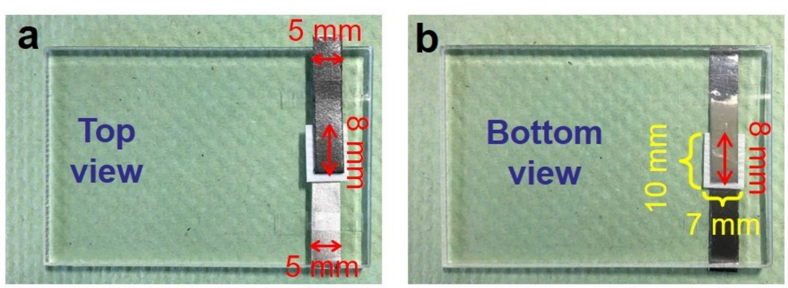

Fig. S5 Display of the prototypical paper-based non-fluidic Al-air battery from top (a) and bottom (b) view. Reaction area for both anode and cathode electrodes are 8×5 mm^2. The size of paper is 10×7 mm^2.

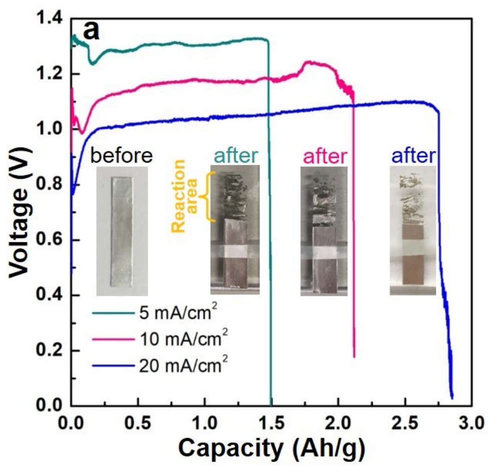

Fig. S6 Discharge curves of paper-based μAl-air battery (a) and non-fluidic Al-air battery (b) under different current density (5, 10, 20 mA/cm^2). The insets are the optical photos of the anode aluminum foil after discharge.

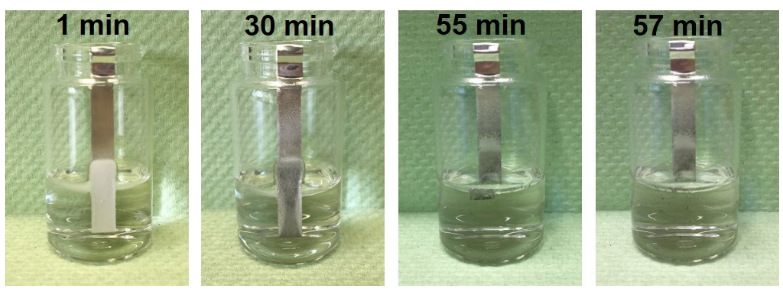

Fig. S7 Aluminum foil (size 8×5 mm^2) immersed in 1.5 M KOH solution.

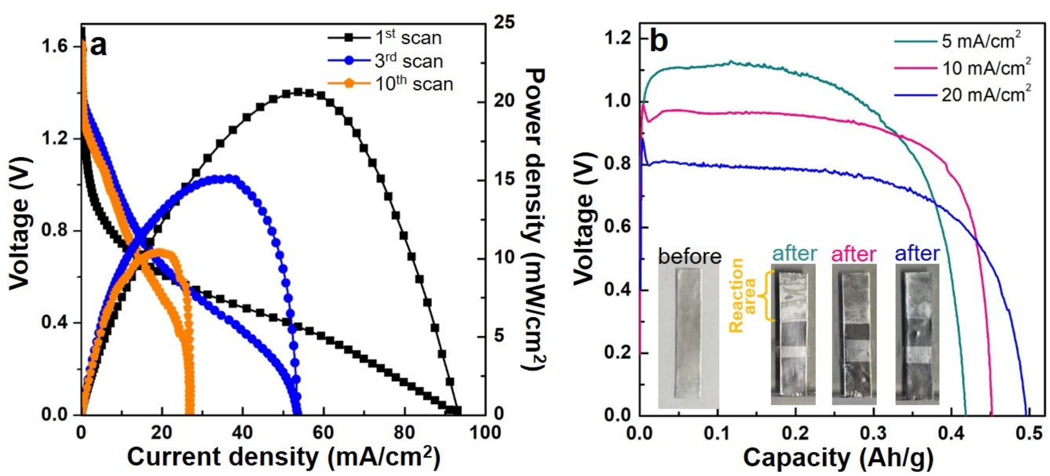

Fig. S8 Performance of non-fluidic Al-air battery using gas diffusion layer air electrode at the cathode. (a) Polarization (*V-I*) and power density curves recorded at different scan numbers. (b) Discharge curves of paper-based and non-fluidic Al-air battery using gas diffusion layer air electrode under different current density (5, 10, 20 mA/cm^2). The insets are the optical photos of the anode aluminum foil after discharge.

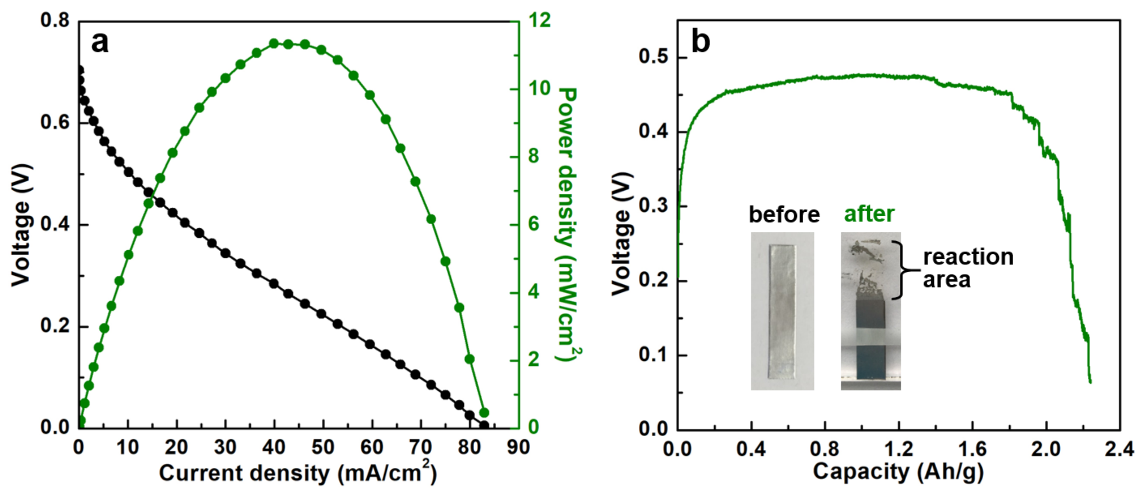

Fig. S9 Polarization (*V-I*) and power density curve (a) and discharge curve (b) of the paper-based µAl-air battery by using 2 M NaCl as electrolyte. The insets are the optical photos of the anode aluminum foil after discharge.

Table S1. Comparisons of the metal-air batteries

Anode	Cathode	Electrolyte	OCV[a] (V)	Maximum Power density (mW/cm^2)	Discharge V (V) @ I (mA/cm^2)[b]	Specific capacity (Ah/g)	Energy density (Wh/kg)	Features	Ref[i]
Al foil	MnO_2 in carbon	$EMIm(HF)_{2.3}F$[c]			1.1@1.5	2.1[f]	2300[f]	Primary Al-air battery with non-aqueous electrolyte	1
Al	N, S doped porous carbon	6 M KOH	1.64	46	0.9@20	0.288	260	Primary Al-air battery	2
Al	$La_{0.7}(Sr_{0.15}Pd_{0.15})MnO_3$	4 M KOH	1.8	265.6	-	-	-	Primary Al-air battery	3
Al	carbon fiber paper supported Ag	4 M NaOH	1.85	109.5	1.56@30	2.78[f]	4340[f]	Primary Al-air battery	4
Carbon treated Al	MnO_2 pasted on Ni mesh	2 M NaCl	-	-	0.4@10	1.2	480	Primary Al-air battery	5
Al mesh	La_2O_3, SrO, MnO_2 and carbon on Ni foam	KOH gel	-	91.13	1.2@18	1.166[f]	1230[f]	All-solid-state battery	6
Ultrafine-grained Al	Ag powder on Ni mesh	2 M NaCl	-	-	0.388@10	2.72[f]	960[f]	Primary Al-air battery	7
		4 M KOH	-	-	1.45@10	2.48[f]	3600[f]		
Al alloy 6061	silver manganate nanoplates loaded air electrode	6 M KOH	1.4	105	0.91@100	2.84[f]	2550[f]	Primary Al-air flow battery (electrolyte flow rate 100 mL/min) controlled by a pump	8
					1.10@50	2.64[f]	2540[f]		
Al wire	MWCNT coated paper	BPS[c]	0.7	0.38[d]	-	-	-	Cable-shaped flexible battery	9
Al spring	Ag coated CNT[c] sheet	Hydrogel PVA[c] KOH	1.7	1.33	1.25@0.5	0.935[f]	1168[f]	All-solid-state, fiber-shape, stretchable battery	10
Al foil	Carbon on steel mesh	1.5 M KOH	1.27	0.6				Disposable, small-size, paper-based battery	11
Al foil	Carbon black	12 wt% NaCl	0.7	0.015	0.54@0.005	0.496[f]	270[f]	Shape-reconfigurable battery	12
						0.128[g]	69[g]		
Al foil	Mn_3O_4/C on carbon paper	SiO_2-modified chitosan hydrogel	1.43	3.8	1.05@1	0.289[f]	303[f]	Al-air coin battery with SiO_2-modified chitosan hydrogel membrane	13

Al foil	Carbon paper	5 M NaOH	1.6	21	0.9@10	1.273[g]	1150[g]	Paper-based Al-air battery with suppressed Al corrosion	14
Al foil	MnO_2/CNT[c] on carbon paper	4 M NaCl	1.5	-	0.6@1	2.462[g]	1480[g]	Paper-based flexible battery	15
Al ink	MnO_2/CNT[c] on paper	4 M NaCl	0.8	-	0.6-0.2@1	0.814[g]	-	Paper-based paintable battery	
Zn film	LaNiO3/NCNT[c]	PVA[c] gelled KOH	1.3	28	1.2@1	0.45[g]	581[g]	Flexible, polymer-electrolyte, rechargeable battery	16
Spiral Zn plate	Fe/N/C on air electrode	alkline gel polymer	1.14	-	0.8@0.1	4.5 Ah/L[h]	3.6 Wh/L[h]	All-solid-state cable-type flexible battery	17
Zn spring	RuO_2 on CNT[c]	Hydrogel polymer	1.29	-	1@1[e]	6 Ah/L[h]	5.7 Wh/L[h]	Rechargeable, flexible, stretchable, fiber-shape battery	18
Zn foil	NCNF[a] film cathode	Alkaline PVA[c] gel	-	-	1.0@2	0.378[f]	378[f]	Flexible battery with good mechanical and cycling stability	19
Zn foil	Co/N/O tri-doped graphene mesh	Alkaline PVA[c] gel	1.45	28	1.19@1.0	-	-	Rechargeable, bendable, flexible, solid battery	20
Zn film	Ultrathin Co_3O_4 on carbon cloth	PVA[c] gel KOH	1.3	17	1.05@2	0.542[f]	546[f]	Flexible thin Zn-air battery	21
Zn plate	$CuCo_2S_4$ nanosheets	PVA[c] gel KOH	1.2	-	1.28@1.0	0.331[f]	424[f]	Flexible all solid Zn-air battery	22
EGILM[a]	Carbon fiber@Pt	PAA[c] gel KOH	1.85	1.25	1.2@0.5	0.21[f]	250[f]	Cable-shaped, soft, elastic, flexible liquid metal-air battery	23
Al foil	Pd/C on graphite foil	1.5 M KOH	1.55	22.5	1.05@20	4.1 Ah/L[h]	4.3 Ah/L[h]	Small, thin, low-cost paper-based µAl-air battery with high power and energy density (electrolyte flow rate 24 µL/min)	This work
					1.05@20	2.75[g]	2900[g]		
					1.17@10	2.11[g]	2470[g]		
					1.30@5	1.47[g]	1910[g]		
		2 M NaCl	0.70	11.3	0.46@20	2.20[g]	1010[g]		

[a]Open circuit voltage
[b]Discharge voltage (V) at discharge current (mA/cm^2)
[c]$EMIm(HF)_{2.3}F$: 1-ethyl-3-methylimidazolium oligo-fluoro-hydrogenate; BPS: phosphate-buffered saline; CNT: carbon nanotubes; NCNT: nitrogen-doped carbon nanotubes; PAA: poly acrylic acid; NCNF: nanoporous carbon nanofiber films; PVA: polyvinyl alcohol; EGILM: Eutectic gallium-indium liquid metal.
[d]0.38 mW/cm.
[e]1 V at 1 A/g.
[f]The capacity and energy density was calculated based on the consumed Al mass.
[g]The capacity and energy density was calculated based on the whole Al mass.
[h]The capacity and energy density was calculated based on the whole volume of the device.
[i]The primary batteries are shown in black text (Ref 1-8). The miniaturized batteries are shown in blue text (Ref 9-23).

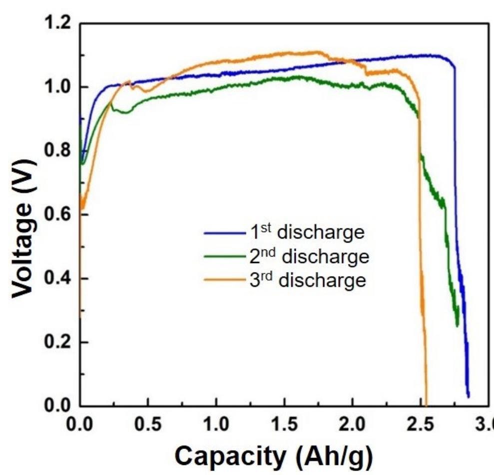

Fig. S10 Mechanically recharging tests. Discharge curves of three paper-based µAl-air battery by using the same cathode electrode.

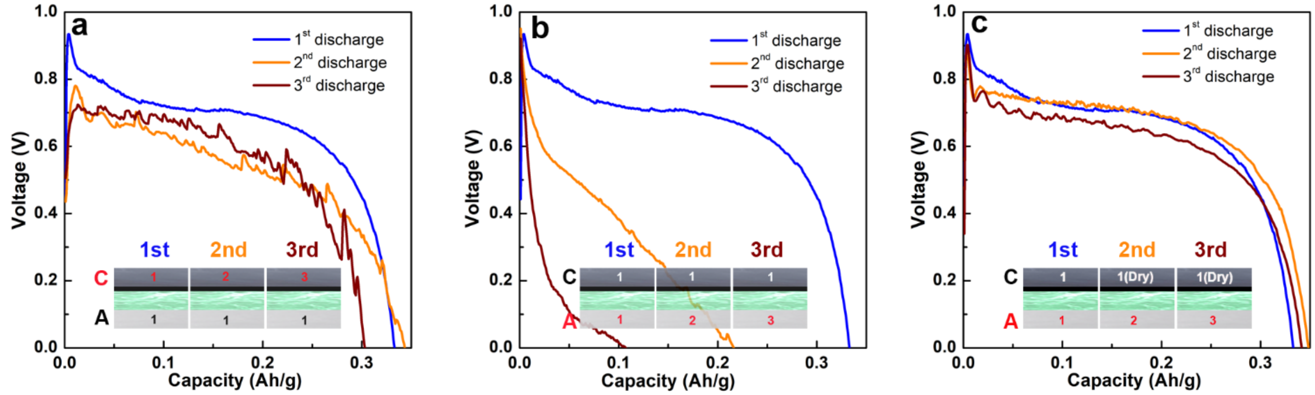

Fig. S11 (a) Discharge curves of three paper-based non-fluidic Al-air battery by using the same anode electrode, but new cathode electrode as well as paper and electrolyte. (b, c) Discharge curves of three paper-based non-fluidic Al-air battery by using the same cathode electrode, but new anode electrode as well as paper and electrolyte; (b) the cathode was used without drying; (c) the cathode was dried in vacuum for 2 h after each discharge, and then reassembled into a non-fluidic Al-air battery for the next discharge.

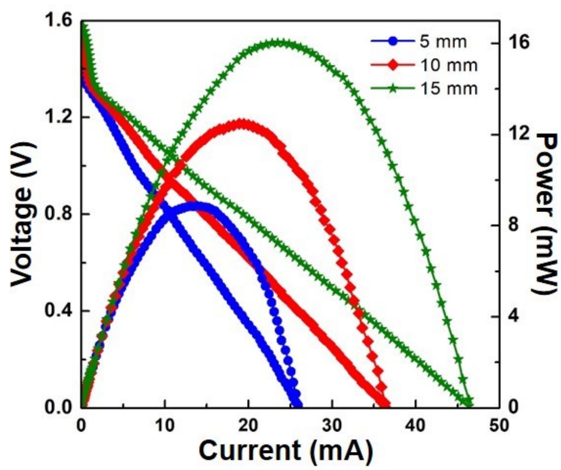

Fig. S12 Polarization (*V-I*) and power density curves of paper-based μAl-air batteries with different electrode sizes.

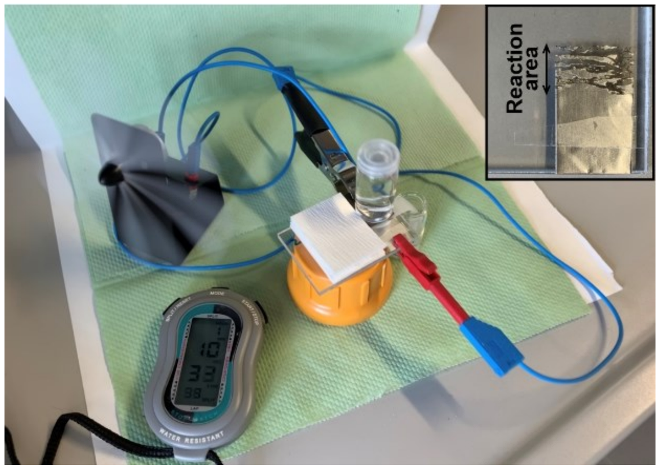

Fig. S13 Running time measurement of a mini-fan (power rating 10 mW) powered by a paper-based μAl-air battery (geometric electrode active area: 8×15 mm^2). The inset shows that after 70 min discharge the Al anode is almost fully consumed.

References

1 D. Gelman, B. Shvartsev, Y. Ein-Eli, *J. Mater. Chem. A*, 2014, **2**, 20237-20242.
2 L. Xu, H. Fan, L. Huang, J. Xia, S. Li, M. Li, H. Ding, K. Huang, *Electrochim. Acta*, 2017, **239**, 1-9.
3 Y. Xue, S. Sun, Q. Wang, H. Miao, S. Li, Z. Liu, *Electrochim. Acta*, 2017, **230**, 418-427.
4 Q. Hong, H. Lu, *Sci. Rep.*, 2017, **7**, 3378.
5 M. Pino, D. Herranz, J. Chacon, E. Fatás, P. Ocón, *J. Power Sources*, 2016, **326**, 296-302.
6 Z. Zhang, C. Zuo, Z. Liu, Y. Yu, Y. Zuo, Y. Song, *J. Power Sources*, 2014, **251**, 470-475.
7 L. Fan, H. Lu, J. Leng, *Electrochim. Acta*, 2015, **165**, 22-28.
8 J. Ryu, H. Jang, J. Park, Y. Yoo, M. Park, J. Cho, *Nat. Commun.*, 2018, **9**, 3715.
9 G. Fotouhi, C. Ogier, J.-H. Kim, S. Kim, G. Cao, A.Q. Shen, J. Kramlich, J.-H. Chung, *J. Micromech. Microeng.*, 2016, **26**, 055011.
10 Y. Xu, Y. Zhao, J. Ren, Y. Zhang, H. Peng, *Angew. Chem.*, 2016, **128**, 8111-8114.
11 A. Avoundjian, V. Galvan, F.A. Gomez, *Micromachines*, 2017, **8**, 222.
12 S. Choi, D. Lee, G. Kim, Y.Y. Lee, B. Kim, J. Moon, W. Shim, *Adv. Funct. Mater.*, 2017, **27**.
13 Y. Liu, Q. Sun, X. Yang, J. Liang, B. Wang, A. Koo, R. Li, J. Li, X. Sun, *ACS Appl. Mater. Interfaces*, 2018, **10**, 19730-19738.
14 Y. Wang, H.Y. Kwok, W. Pan, H. Zhang, X. Lu, D.Y. Leung, *Appl. Energ.*, 2019, **251**, 113342.
15 Y. Wang, H. Kwok, W. Pan, H. Zhang, D.Y. Leung, *J. Power Sources*, 2019, **414**, 278-282.
16 J. Fu, D.U. Lee, F.M. Hassan, L. Yang, Z. Bai, M.G. Park, Z. Chen, *Adv. Mater.*, 2015, **27**, 5617-5622.
17 J. Park, M. Park, G. Nam, J.s. Lee, J. Cho, *Advanced Materials*, 2015, **27**, 1396-1401.
18 Y. Xu, Y. Zhang, Z. Guo, J. Ren, Y. Wang, H. Peng, *Angew. Chem. Int. Ed.*, 2015, **54**, 15390-15394.
19 Q. Liu, Y. Wang, L. Dai, J. Yao, *Advanced Materials*, 2016, **28**, 3000-3006.
20 C. Tang, B. Wang, H.F. Wang, Q. Zhang, *Adv. Mater.*, 2017, **29**, 1703185.
21 X. Chen, B. Liu, C. Zhong, Z. Liu, J. Liu, L. Ma, Y. Deng, X. Han, T. Wu, W. Hu, *Adv. Energy Mater.*, 2017, **7**, 1700779.
22 Y. Li, J. Yin, L. An, M. Lu, K. Sun, Y.-Q. Zhao, F. Cheng, P. Xi, *Nanoscale*, 2018, **10**, 6581-6588.
23 G. Liu, J.Y. Kim, M. Wang, J.Y. Woo, L. Wang, D. Zou, J.K. Lee, *Adv. Energy Mater.*, 2018, 1703652.